

L16 Orthogonal Design Synthesis of NASICON-Type $\text{Li}_{1.4}\text{Al}_{0.4}\text{Ti}_{1.6}(\text{PO}_4)_3$ Solid Electrolyte by Pechini Method for Process Optimization

M. R. Ghaani and P. Marashi*

* pmarashi@aut.ac.ir

Received: January 2018

Accepted: April 2018

Department of Mining and Metallurgical Engineering, Amirkabir University of Technology, Tehran, Iran

DOI: 10.22068/ijmse.15.3.60

Abstract: Na super ionic conductive (NASICON) materials are ceramics with three-dimensional scaffolds. In this study, $\text{Li}_{1.4}\text{Al}_{0.4}\text{Ti}_{1.6}(\text{PO}_4)_3$ with NASICON structure was synthesized by Pechini method. As a result, a sample having a total conduction of $1.18 \times 10^{-3} \text{ S cm}^{-1}$ was attained. In addition, various parameters were studied to obtain high value of conductivity, by optimizing the process. The optimization was made using L16 Taguchi based orthogonal array, followed by ANOM, ANOVA and stepwise regression. As a result, the optimum synthesis parameters can be obtained, while pH of the solution was adjusted to 7. The ratio between the concentration of citric acid to metal ions and ethylene glycol concentration stuck to 1 and 2.5, respectively. The best heat treatment can be carried out with a combination of pyrolysis at 600 °C and sintering at 1000 °C.

Keywords: L16 Orthogonal Array, NASICON, Pechini, Ionic Conductivity, ANOM, Stepwise Regression, Electrochemical Impedance spectroscopy, LTP, Peroxotitanium.

1. INTRODUCTION

During the last decade solid lithium ion conductors have found widespread applications in areas such as high-energy lithium ion batteries [1-3], electrochemical sensors [4-6] and supercapacitors [7] due to their high ionic conductivity and relatively high chemical stability [8, 9]. Sodium superionic conductor (NASICON), with a 3D framework structure, is compound as a major fast ionic conduction compound.

Various methods for the synthesis of this ceramic compound such as sol-gel [10-12], solid state [13-15] and melt quenching [16-18] process have been used. Sol-gel has several advantages, such as: much lower processing temperatures, a high homogeneity of the resulting structures, the possibility of obtaining pure phase of multi-component metal oxides [19], low manufacturing cost, simple stoichiometry control, and fast deposition rate [20]. Generally Alkoxides as organometallic reagents [21, 22] or soluble metallic salts (used in Pechini method) [23-25], have applied for sol-gel synthesis of this structure. However, the main disadvantage of

alkoxides is their extreme sensitivity to moisture and a high reactivity toward hydrolysis, which affect the hydroxylation process [26].

Pechini process consists of two combined stages; a process of forming metal complexes and in situ polymerization of organic compounds [27]. In general, hydroxycarboxylic acids are used to form stable metal complexes. The polyesterification of metal complexes is reached using a polyhydroxy alcohol and finally a rigid organic polymer is produced. Immobilization of metal complexes in this rigid polymeric network ensures the compositional homogeneity. Thereafter, the polymeric resin is calcinated and a pure phase of multi-component metal oxides is attained [28].

Xu et al. (2007) demonstrated that using citric acid-assisted sol-gel process, it is possible to obtain well crystallized glass-ceramics of $\text{Li}_{1.4}\text{Al}_{0.4}\text{Ti}_{1.6}(\text{PO}_4)_3$ at a much lower temperature in a shorter synthesis time compared to the conventional solid-state method. They reported that the optimized conditions for citrate-based manufacturing process are: the molar ratio of [citric acid + ethylene glycol] / $[\text{Li}^{+} + \text{Al}^{3+} + \text{Ti}^{4+}] = 4$ and pH = 7 [19]. Additionally, Mariappan et al.

(2006) successfully prepared NASICON-type nanostructured material by a Pechini like polymerizable complex method. The optimum conditions of the synthesis process were [ethylene glycol]/[citric acid]= 1 with calcination of the powder precursor in the temperature range of 650 to 1050 °C [26]. However, a review of the literature shows that there are few reports on the effect of important parameters of Pechini synthesis on the electrical property of NASICON materials.

Moreover, the investigation of relevant factors in synthesis processes has traditionally been carried out by taking into account the factors in isolation and the 'one factor at a time' methodology which is not considered efficient design strategy. An appropriate approach is to apply one of the proposed experimental design methods such as factorial, response surface methodology, Taguchi and etc. [29-32]. These techniques are able to simultaneously view on a number of factors at different levels; however, such approach is hardly observed for the synthesis purposes. While in a synthesis process, such as sol-gel, there is a complex chemistry and there are several series of efficient parameters. Therefore, to achieve the desired properties as a result of optimization in synthesis conditions, the use of experimental design is critical.

The aim of this study is investigating the effect of some important parameters including citric acid to metallic ions ratio, pH, citric acid to ethylene glycol ratio, calcination and sintering temperatures on the Pechini synthesis of NASICON type ceramic employing design of experiments. In addition, the optimum synthesis conditions and a mathematical model for the conductivity value as a function of synthesis parameters are provided. Electrochemical impedance spectroscopy and X-ray diffraction analysis are used to characterize the properties of the final product obtained.

2. EXPERIMENTAL

Li_2CO_3 (Sigma-Aldrich), Ti powder, $\text{Al}(\text{NO}_3)_3 \cdot 9\text{H}_2\text{O}$ and $\text{NH}_4\text{H}_2\text{PO}_4$ (Merck) were used in the synthesis of $\text{Li}_{1.4}\text{Al}_{0.4}\text{Ti}_{1.6}(\text{PO}_4)_3$ powder (LATP). In the early stage, peroxotitanium solution was prepared by

dissolving Ti metal powder (Sigma-Aldrich, 99.98%) in hydrogen peroxide (Merck, 30%) and ammonia (Merck, 25%). To prevent the precipitation of Titanium hydroxide and achieving a stable, transparent sol, citric acid is added. [33]. Further, a solution of lithium carbonate, ammonium dihydrogen phosphate and ethylene glycol (EG) (Sigma-Aldrich, >99%) was added to make the final solution. The esterification reaction at 80 °C after 3 hours transfers the sol into a solid, rigid gel. The final product will be prepared by two steps of heat treatment on the formed gel. Both calcination and sintering procedures were carried out using an aluminum crucible in a Carbolite tube furnace (air atmosphere) with a heating rate of 2 °C min^{-1} up to the final temperatures, the samples were 2 h. The synthesis procedure is illustrated in Fig. 1.

Phase analysis was performed by X-ray diffraction, XRD, (Bruker D8) using Cu-K α radiation ($\lambda=1.5419\text{\AA}$) over the 2θ range of 10°-70° in 0.02° steps. To measure the ion conductivity, cylindrical disks with 13mm diameter and 2mm thickness were prepared and silver ink was used to make the blocking electrodes at both sides of the pellets. The complex impedance measurements were performed using Autolab impedance analyzer over the frequency range of 1–106 Hz at 50 points.

According to previous studies pH, CA/M and CA/EG ratios of the prepared sol, as well as calcining and sintering temperatures were selected as the most effective parameters in our selected synthesis method [19, 26, 34]. Where M is the total moles of metallic ions present in the solution.

The L16 orthogonal array of Taguchi method [35] was used in order to optimize the results and find out the most important parameters. Then ANOVA was used to determine the effectiveness of each parameter on the conduction through grains and grain boundaries. Regression analysis is carried out to find the optimum synthesis conditions by using stepwise backward elimination in order to obtain maximum ionic conductivity.

To define each factor the L16 array must be evaluated in four levels (Table 1) in a range that is selected based on the earlier literature [19, 26]. L16 proposes 16 different runs with different combinations of each selected factors (Table 2).

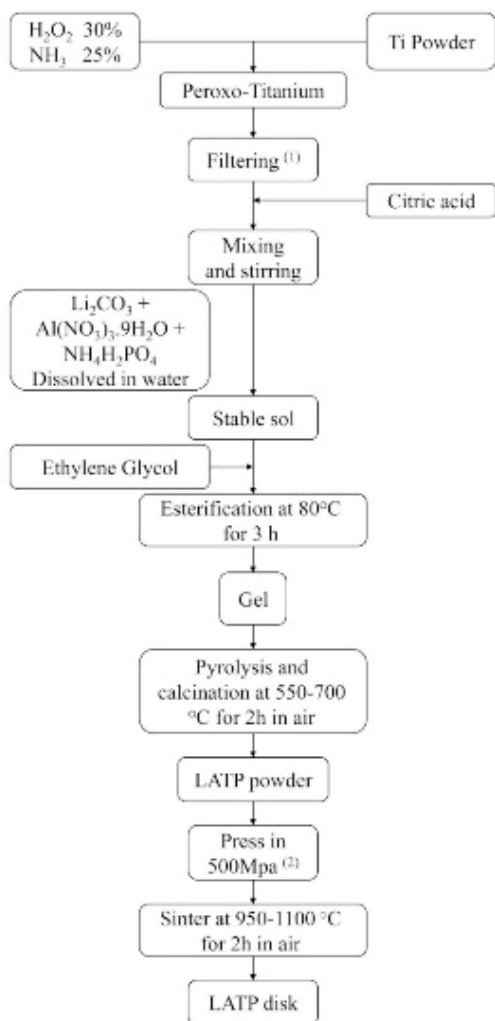


Fig. 1. The Pechini synthesis of NASICON type structure.
 (1) The filtering step is to remove unreacted titanium powders from the solution. Afterward the citric acid has to be added immediately to stop titanium to react with water.
 (2) No additional binder was used for the disk preparation.

Table 1. The defined values for each level of studied parameters. M is the total moles of metallic ions present in the solution.

pH	CA/M	CA/EG	$T_{cal.}(^{\circ}C)$	$T_{sin.}(^{\circ}C)$
5	0.75	0.5	550	1100
6	1	1	600	950
7	1.5	2	650	1000
8	2	2.5	700	1050

Table 2. The proposed runs based on the L16 orthogonal design

Run	pH	CA/M	CA/EG	$T_{cal.}(^{\circ}C)$	$T_{sin.}(^{\circ}C)$
1	5	0.75	1	550	1100
2	5	1	1.5	600	950
3	5	0.5	2	650	1000
4	5	2	2.5	700	1050
5	6	0.75	1.5	650	1050
6	6	1	1	700	1000
7	6	0.5	2.5	550	950
8	6	2	2	600	1100
9	7	0.75	2	700	950
10	7	1	2.5	650	1100
11	7	0.5	1	600	1050
12	7	2	1.5	550	1000
13	8	0.75	2.5	600	1000
14	8	1	2	550	1050
15	8	0.5	1.5	700	1100
16	8	2	1	650	950

3. RESULTS AND DISCUSSION

3.1. Electrochemical Impedance Spectroscopy Studies

A typical recorded Nyquist diagram for the 16 samples is illustrated in Fig. 2. The R_i values of each tested sample, were determined from the simulated Nyquist plots as shown in Figure 2. The equivalent circuit for the assembly consists of pure resistance (R_0 and R_1) and a constant phase element (CPE_e and CPE_1). There is no doubt that $R_0 + R_1$ is the total resistance (R_{total}) of the sample. However, there are some arguments about the determination of grain and grain-boundary resistance (R_b and R_{gb}). Several reports directly attributed R_0 to the resistance of ion migration in the mass of LATP; while, R_1 was attributed to the grain boundary of the LATP plate [36-39].

To compare the data from different samples, the conductivity value of each sample was calculated using the following equation. As a result, the final value was corrected with regards to the dimensional differences of the samples.

$$\sigma_i = 4t / (\pi D^2 R_i)$$

where σ_i and R_i are the conductivity and the resistance of component i , and t and D are

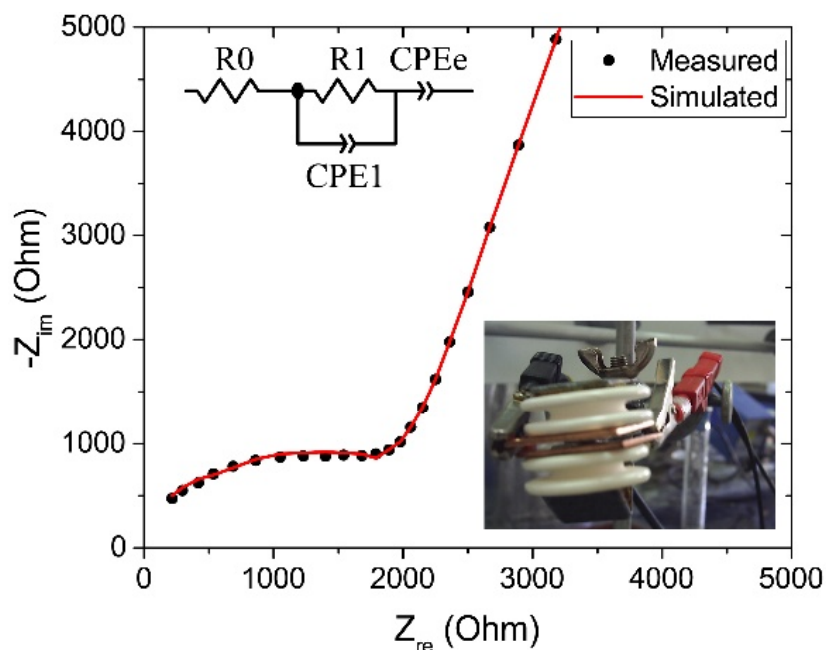


Fig. 2. A typical recorded Nyquist plot along with the simulated curve using the presented equivalent circuit. R0 and R1 represents the resistance of grain and the grain boundary respectively. A handmade setup was used to measure the impedance in solid state mode. Silver ink was applied on both sides of the prepared disk to have electrodes with a good contact. Two copper plates were delivered the electricity from the instrument connections to the coated electrodes while a same amount of pressure was applied to tighten the cell. 50 logarithmically spaced points were recorded for each sample in the frequency range of 1–106 Hz at room temperature.

Table 3. Calculated conductivity values base on the recorded electrochemical impedance spectra of each samples. σ_{total} =total conductivity, σ_g = grain conductivity and σ_{gb} = grain boundary conductivity. All the values are normalized concerning the electrode area and the thickness of the disk.

Run	σ_{total} (S.cm ⁻¹)	σ_b (S.cm ⁻¹)	σ_{gb} (S.cm ⁻¹)
1	2.5×10^{-5}	8.3×10^{-3}	2.6×10^{-5}
2	3.5×10^{-5}	3.9×10^{-3}	3.6×10^{-5}
3	7.0×10^{-5}	4.4×10^{-2}	7.0×10^{-5}
4	9.6×10^{-6}	4.0×10^{-3}	9.6×10^{-6}
5	4.3×10^{-5}	5.5×10^{-3}	4.3×10^{-5}
6	5.5×10^{-5}	1.9×10^{-3}	5.6×10^{-5}
7	4.7×10^{-5}	2.7×10^{-2}	4.9×10^{-5}
8	3.9×10^{-5}	8.0×10^{-3}	3.9×10^{-5}
9	1.3×10^{-5}	4.2×10^{-2}	1.3×10^{-5}
10	1.5×10^{-4}	1.8×10^{-2}	1.5×10^{-4}
11	1.1×10^{-4}	3.3×10^{-2}	1.1×10^{-4}
12	1.6×10^{-5}	1.6×10^{-2}	1.6×10^{-5}
13	1.0×10^{-4}	6.7×10^{-2}	1.0×10^{-4}
14	3.5×10^{-5}	2.0×10^{-2}	3.5×10^{-5}
15	4.2×10^{-5}	1.2×10^{-3}	4.3×10^{-5}
16	2.4×10^{-6}	3.4×10^{-4}	2.5×10^{-6}

thickness and diameter of the analyzed disk, respectively. The values of the total conductivity (σ_{total}), the conductivity of the grains (σ_b) and the conductivity of the grain boundaries (σ_{gb}) are listed in Table 3.

Based on the fact that the resistance of grains and grain boundaries behave like a serial circuit ($R_{total}=R_b+R_{gb}$), and taking into account the conductivity values (Table 2), it can be concluded that the rate limiting step of ion migration in this conductive system is the conduction through the grain boundaries.

The results of Table 3 reveal that samples 10 and 11 are evaluated as the two most conductive samples. Although the grain conductivity for sample 11 is higher, the ions migrate faster through grain boundaries of sample 10. Consequently, sample No. 10 is performed as the most conductive sample among all others in this study. Fig. 3 shows a schematic comparison of three possible conductivity classes between these two samples.

- Sub-ppm H₂S sensor based on NASICON and CoCr_{2-x}MnxO₄ sensing electrode, RSC Advances, 2014, 4, 55334-55340.
6. P. Lorenc, A. Strzelczyk, B. Chachulski, G. Jasinski, Properties of Nasicon-based CO₂ sensors with Bi₈Nb₂O₁₇ reference electrode, Solid State Ionics, 2015, 271, 48-55.
 7. K. M. Hercule, Q. Wei, O. K. Asare, L. Qu, A. M. Khan, M. Yan, C. Du, W. Chen, L. Mai, "Interconnected nanorods-nanoflakes Li₂Co₂(MoO₄)₃ framework structure with enhanced electrochemical properties for supercapacitors", Advanced Energy Materials, 2015, 5 .
 8. N. Gorodylova, V. Kosinová, Ž. Dohnalová, P. Šulcová, P. Bělina, "Thermal stability and colour properties of CuZr₄(PO₄)₆", Journal of Thermal Analysis and Calorimetry, 2016, 1-8.
 9. Y. Shimizu, T. Ushijima, "Sol-gel processing of NASICON thin film using aqueous complex precursor", Solid State Ionics, 2000, 132, 143-148.
 10. R. Klee, P. Lavela, M. J. Aragón, R. Alcántara, J. L. Tirado, "Enhanced high-rate performance of manganese substituted Na₃V₂(PO₄)₃/C as cathode for sodium-ion batteries", Journal of Power Sources, 2016, 313, 73-80.
 11. S. Kumar, P. Balaya, "Improved ionic conductivity in NASICON-type Sr²⁺ doped LiZr₂(PO₄)₃", Solid State Ionics, 2016, 296, 1-6.
 12. F. Ma, E. Zhao, S. Zhu, W. Yan, D. Sun, Y. Jin, C. Nan, "Preparation and evaluation of high lithium ion conductivity Li_{1.3}Al_{0.3}Ti_{1.7}(PO₄)₃ solid electrolyte obtained using a new solution method", Solid State Ionics, 2016, 295, 7-12.
 13. S. Kim, V. Mathew, J. Kang, J. Gim, J. Song, J. Jo, J. Kim, "High rate capability of LiFePO₄ cathodes doped with a high amount of Ti," Ceramics International, 2016, 42, 7230-7236.
 14. D.H. Kothari, D. K. Kanchan, "Effect of doping of trivalent cations Ga³⁺, Sc³⁺, Y³⁺ in Li_{1.3}Al_{0.3}Ti_{1.7}(PO₄)₃ (LATP) system on Li⁺ ion conductivity", Physica B: Condensed Matter, 2016, 501, 90-94.
 15. D. H. Kothari, D. K. Kanchan, "Study of Li⁺ conduction in Li_{1.3}Al_{0.3-x}Sc_xTi_{1.7}(PO₄)₃ (x=0.01, 0.03, 0.05 and 0.07) NASICON ceramic compound", Physica B: Condensed Matter, 2016, 494, 20-25.
 16. M. Y. Hassaan, Z. Kaixin, J. Wang, M. G. Moustafa, "Mössbauer and electrical conduction investigations of LiFe(BaTi)(PO₄) NASICON nano composite", Hyperfine Interactions, 2016, 237, 1-15.
 17. M. Y. Hassaan, S. M. Salem, M. G. Moustafa, S. Kubuki, K. Matsuda, T. Nishida, "Controlled crystallization a ionic conductivity of nanostructured LiNbFePO₄ glass ceramic", Hyperfine Interactions, 2014, 226, 131-140.
 18. M. Illbeigi, A. Fazlali, M. Kazazi, A. H. Mohammadi, "Effect of simultaneous addition of aluminum and chromium on the lithium ionic conductivity of LiGe₂(PO₄)₃ NASICON-type glass-ceramics", Solid State Ionics, 2016, 289, 180-187.
 19. X. Xu, Z. Wen, J. Wu, X. Yang, "Preparation and electrical properties of NASICON-type structured Li_{1.4}Al_{0.4}Ti_{1.6}(PO₄)₃ glass-ceramics by the citric acid-assisted sol-gel method", Solid State Ionics, 2007, 178, 29-34.
 20. K. Dokko, K. Hoshina, H. Nakano, K. Kanamura, "Preparation of LiMn₂O₄ thin-film electrode on Li_{1+x}Al_xTi_{2-x}(PO₄)₃ NASICON-type solid electrolyte", Journal of Power Sources, 2007, 174, 1100-1103.
 21. E. Christensen, J. H. Von Barner, J. Engell, N. J. Bjerrum, "Preparation of CuZr₂P₃O₁₂ from alkoxide-derived gels: phase formation as a function of heat treatment", Journal of Materials Science, 1990, 25, 4060-4065.
 22. N. S. Bell, C. Edney, J. S. Wheeler, D. Ingersoll, E. D. Spoerke, "The influences of excess sodium on low-temperature NaSICON synthesis", Journal of the American Ceramic Society, 2014, 97, 3744-3748.
 23. F. Ejehi, S. P. H. Marashi, M. R. Ghaani, D. F. Haghshenas, "The synthesis of NaSICON-type ZrNb(PO₄)₃ structure by the use of Pechini method", Ceramics International, 2012, 38, 6857-6863.
 24. V. Aravindan, M. Ulaganathan, W. C. Ling, S. Madhavi, "Fabrication of New 2.4V Lithium-Ion Cell with Carbon-Coated LiTi₂(PO₄)₃ as the Cathode", ChemElectroChem, 2015, 2, 231-235.
 25. E. Zhao, F. Ma, Y. Jin, K. Kanamura, "Pechini synthesis of high ionic conductivity

- Li_{1.3}Al_{0.3}Ti_{1.7}(PO₄)₃ solid electrolytes: The effect of dispersant”, *Journal of Alloys and Compounds*, 2016, 680, 646-653.
26. C. R. Mariappan, C. Galven, M. P. Crosnier-Lopez, F. Le Berre, O. Bohnke, “Synthesis of nanostructured LiTi₂(PO₄)₃ powder by a Pechini-type polymerizable complex method”, *Journal of Solid State Chemistry*, 2006, 179, 450-456.
 27. M. A. Gomes, Á. S. Lima, K. I. B. Eguiluz, G. R. Salazar-Banda, “Wet chemical synthesis of rare earth-doped barium titanate nanoparticles”, *Journal of Materials Science*, 2016, 51, 4709-4727.
 28. D. Segal, “Chemical synthesis of ceramic materials”, *Journal of Materials Chemistry*, 1997, 7, 1297-1305.
 29. A. Akrami, A. Niazi, “Synthesis of maghemite nanoparticles and its application for removal of Titan yellow from aqueous solutions using full factorial design”, *Desalination and Water Treatment*, 2016, 57, 22618-22631.
 30. S. J. Park, H. K. An, “Optimization of fabrication parameters for nanofibrous composite membrane using response surface methodology”, *Desalination and Water Treatment*, 2016, 57, 20188-20198.
 31. B. A. E. Ben-Arfa, I. M. M. Salvado, J. R. Frade, R. C. Pullar, “Fast route for synthesis of stoichiometric hydroxyapatite by employing the Taguchi method”, *Materials and Design*, 2016, 109, 547-555.
 32. H. Toshiyoshi, T. Konishi, K. Machida, K. Masu, “A mixed-design technique for integrated MEMS using a circuit simulator with HDL”, *Proceedings of the 20th International Conference on Mixed Design of Integrated Circuits and Systems, MIXDES 2013*, 2013, pp. 17-22.
 33. M. Natsume, J. H. Kim, S. Yonezawa, M. Takashima, “Preparation and characterization of nano-sized BaTiO₃ particles using aqueous peroxotitanium acid solution: Effects of pH adjustment”, *Materials Chemistry and Physics*, 2014, 148, 169-174.
 34. M. Hajizadeh-Oghaz, R. Shoja Razavi, M. “Khajelakzay, Optimizing sol-gel synthesis of magnesia-stabilized zirconia (MSZ) nanoparticles using Taguchi robust design for thermal barrier coatings (TBCs) applications”, *Journal of Sol-Gel Science and Technology*, 2014, 73, 227-241.
 35. R. Roy, “Design Of Experiment using the Taguchi approach”, Wiley Interscience 2001.
 36. C.R. Gautam, D. Kumar, P. Singh, O. Parkash, Study of Impedance Spectroscopy of Ferroelectric (Pb Sr)TiO₃ Glass Ceramic System with Addition of La₂O₃, *ISRN Spectroscopy*, 2012, 11.
 37. J. S. Lee, C. M. Chang, Y. I. L. Lee, J. H. Lee, S. H. Hong, “Spark Plasma Sintering (SPS) of NASICON Ceramics”, *Journal of the American Ceramic Society*, 2004, 87, 305-307.
 38. A. Ahmad, T. A. Wheat, A. K. Kuriakose, J. D. Canaday, A. G. McDonald, “Dependence of the properties of Nasicons on their composition and processing”, *Solid State Ionics*, 1987, 24, 89-97.
 39. Y. Noguchi, E. Kobayashi, L. S. Plashnitsa, S. Okada, J. i. Yamaki, “Fabrication and performances of all solid-state symmetric sodium battery based on NASICON-related compounds”, *Electrochimica Acta*, 2013, 101 59-65.
 40. X. Xu, Z. Wen, X. Yang, L. Chen, “Dense nanostructured solid electrolyte with high Li-ion conductivity by spark plasma sintering technique”, *Materials Research Bulletin*, 2008, 43, 2334-2341.
 41. E. Kazakevicius, A. Urcinskas, A. Kezionis, A. Dindune, Z. Kanepė, J. Ronis, “Electrical properties of Li_{1.3}Ge_{1.4}Ti_{0.3}Al_{0.3}(PO₄)₃ superionic ceramics”, *Electrochimica Acta*, 2006, 51, 6199-6202.
 42. K. Arbi, M. G. Lazarraga, D. Ben Hassen Chehimi, M. Ayadi-Trabelsi, J. M. Rojo, J. Sanz, “Lithium Mobility in Li_{1.2}Ti_{1.8}R_{0.2}(PO₄)₃ Compounds (R = Al, Ga, Sc, In) as Followed by NMR and Impedance Spectroscopy”, *Chemistry of Materials*, 2003, 16, 255-262.
 43. K. Arbi, J. M. Rojo, J. Sanz, “Lithium mobility in titanium based Nasicon Li_{1+x}Ti_{2-x}Al_x(PO₄)₃ and LiTi_{2-x}Zr_x(PO₄)₃ materials followed by NMR and impedance spectroscopy”, *Journal of the European Ceramic Society*, 2007, 27, 4215-4218.
 44. M. S. Phadke, “Quality Engineering Using Robust Design”, Prentice Hall, 1989.
 45. D. L. Tran, Q. Q. Ngo, Cathode materials for rechargeable Li-ion batteries: Sol-Gel synthesis

- and characterization of LiMn_2O_4 and $\text{LiCu}_x\text{Mn}_{2-x}\text{O}_4$, 2004
46. S. G. Rudisill, N. M. Hein, D. Terzic, A. Stein, "Controlling Microstructural Evolution in Pechini Gels through the Interplay between Precursor Complexation", *Step-Growth Polymerization, and Template Confinement, Chemistry of Materials*, 2013, 25, 745-753.
 47. F. Acosta-Humánez, O. Almanza, C. Vargas-Hernández, "Effect of sintering temperature on the structure and mean crystallite size of $\text{Zn}_{1-x}\text{Co}_x\text{O}$ ($x = 0.01 - 0.05$) samples", *Superficies y Vacío*, 2014, 27, 43-48.
 48. Q. Ma, M. Guin, S. Naqash, C. L. Tsai, F. Tietz, O. Guillon, "Scandium-Substituted $\text{Na}_3\text{Zr}_2(\text{SiO}_4)_2(\text{PO}_4)$ Prepared by a Solution-Assisted Solid-State Reaction Method as Sodium-Ion Conductors", *Chemistry of Materials*, 2016, 28, 4821-4828.
 49. I. S. Fahim, S. M. Elhaggar, H. Elayat, "Experimental Investigation of Natural Fiber Reinforced Polymers", *Materials Sciences and Applications*, 2012, 03, 4.
 50. A. M. Alshaibani, Z. Yaakob, A. M. Alsobaai, M. Sahri, "Optimization of $\text{Pd-B}^{1/3}\text{-Al}_2\text{O}_3$ catalyst preparation for palm oil hydrogenation by response surface methodology (RSM)", *Brazilian Journal of Chemical Engineering*, 2014, 31, 69-78.
 51. C. Davis, J. C. Nino, "Microwave Processing for Improved Ionic Conductivity in $\text{Li}_2\text{O-Al}_2\text{O}_3\text{-TiO}_2\text{-P}_2\text{O}_5$ Glass-Ceramics", *Journal of the American Ceramic Society*, 2015, 98, 2422-2427.
 52. K. Arbi, W. Bucheli, R. Jiménez, J. Sanz, "High lithium ion conducting solid electrolytes based on NASICON $\text{Li}_{1+x}\text{Al}_x\text{M}_{2-x}(\text{PO}_4)_3$ materials ($M = \text{Ti, Ge}$ and $0 \leq x \leq 0.5$)", *Journal of the European Ceramic Society*, 2015, 35, 1477-1484.
 53. K. Waetzig, A. Rost, U. Langklotz, B. Matthey, J. Schilm, "An explanation of the microcrack formation in $\text{Li}_{1.3}\text{Al}_{0.3}\text{Ti}_{1.7}(\text{PO}_4)_3$ ceramics", *Journal of the European Ceramic Society*, 2016, 36, 1995-2001